ACS OMEGA

http://pubs.acs.org/journal/acsodf

Article

Electrostatic Fields Promote Methanogenesis More than Polarized Bioelectrodes in Anaerobic Reactors with Conductive Materials

Hanchao Yu, Young-Chae Song,* Byung-Uk Bae, Jun Li, and Seong-Ho Jang

Cite This: *ACS Omega* 2021, 6, 29703−29712

Read Online

ACCESS | Metrics & More | Article Recommendations

ABSTRACT: Direct interspecies electron transfer (DIET) is a breakthrough that can surpass the limitations of anaerobic digestion. Conductive materials and polarized bioelectrodes are known to induce DIET for methane production but are still challenging to apply at a field scale. Herein, compared to polarized bioelectrodes, electrostatic fields that promote DIET were investigated in an anaerobic reactor with conductive materials. As a conductive material, activated carbon enriched its surface with electroactive microorganisms to induce DIET (cDIET). cDIET improved the methane yield to 254.6 mL/g COD_r, compared to the control. However, polarized bioelectrodes induced electrode-mediated DIET and biological DIET (bDIET), in addition to cDIET, improving the methane yield to 310.7 mL/g COD_r. Electrostatic fields selectively promoted bDIET and cDIET for further methane production compared to the polarized bioelectrodes. As the contribution of DIET increased, the methane yield increased, and the substrate residue decreased, resulting in a significant improvement in methane production.

INTRODUCTION

Anaerobic digestion is a series of microbial metabolic processes that decompose and stabilize organic matter in an oxygen-free environment and produce methane as a byproduct. In the anaerobic metabolic processes, acidogenic bacteria break down organic matter and transfer the electrons to the intermediates, such as acetate and hydrogen. Then, methanogenic archaea convert the electrons from the intermediates into methane. Thus, anaerobic digestion is an indirect interspecies electron transfer (IIET) process via intermediates from organic matter to methane.[1−3] However, methanogenic archaea have physiological properties that are different from those of acidogenic bacteria.[4,5] Thereby, the intermediates in anaerobic digestions can be quickly accumulated by disturbing the balance between their production and consumption, even with minor changes in environments such as pH and temperature.[3,6] In addition, due to thermodynamic limitations, the intermediates cannot be entirely converted to methane, and some of the intermediates with low solubility or high volatility can be released into the gaseous phase.[5] Acidogenesis and methanogenesis, in particular, are multiple enzymatic reactions with inevitable energy losses.[2,5,7] Therefore, the methane yield of organic matter is generally lower than the theoretical value.

In recent years, direct interspecies electron transfer (DIET) between electroactive microorganisms (EAM) has received considerable attention as a key to overcoming the limitations of anaerobic digestion.[5,8] The microbial groups of EAM for methane production include exoelectrogenic bacteria (EEB) and electrotrophic methanogenic archaea (EMA). EEB is the bacterial species that is capable of transferring electrons directly outside the cells through C-type cytochromes or conductive pili.[2,4,7,9] EMA can produce methane by directly accepting the electrons from EEB without the intermediates.[8,10] In general, the types of DIET for methane production are classified as follows: (i) conductive material-mediated DIET (cDIET), (ii) electrode-mediated DIET (eDIET), and biological DIET (bDIET) between EEB and EMA electrically connected by physical contact.[1,5,9] DIET is advantageous in kinetics over IIET and conserves electrons better.[2,7] Therefore, the anaerobic digestion process can be more stable and robust, as DIET contributes more to methane production.[5,11] DIET can be induced by enriching EAM, and providing the driving force for the electron transfer. EAM can be naturally enriched when insoluble electron acceptors are outside the cells in anaerobic or nutrient-limited environments.[12,13] However, conductive materials and polarized bioelectrodes can also enrich their surfaces with EAM in the anaerobic condition, driving cDIET and eDIET, respectively.[14,15] In anaerobic

Received: August 1, 2021
Accepted: October 21, 2021
Published: October 29, 2021

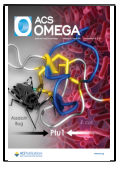

digestion, various conductive materials such as activated carbon, metal oxide, carbon fiber, and metal-conductive polymer composites significantly promoted methane production through cDIET.[16,17] It has been understood that cDIET from EAM to EMA through conductive materials promotes methane production by reducing carbon dioxide.[4,8] However, recent reports suggest that conductive materials also promote acetate dismutation for methane production.[17−19] The conductive materials with electrochemical activity, such as nanocarbon compounds based on a carbon nanotube and graphene, metal−organic framework, and metal-polyelectrolyte complexes, appear to have the potential to enhance methane production further.[20−24] Microbial electrolysis cells (MECs) are examples of polarized bioelectrodes that enrich the electrode surface with EAM, promoting eDIET for hydrogen or methane production.[25−27] However, the methane production in the anaerobic digestion combined with MECs could only be improved satisfactorily by providing polarized bioelectrodes of a sufficient surface area.[5]

It is worth noting that electrostatic fields move electrons, polar molecules, and charged ions by the Lorentz force.[28] The Lorentz force may promote DIET for methane production under electrostatic fields. There are several reports that electrostatic fields promote the redox reaction in the biological process. The polarized bioelectrode installed in an upflow anaerobic reactor significantly improved methane production, while the eDIET contributed only a few percentage points.[29,30] The performances of aerobic composting and biological nitrogen removal processes were also improved under electrostatic fields, and their bulk medium showed bioelectrochemical activities.[31−33] Direct evidence that electrostatic fields promote DIET for methane production was observed from the conversion process of lignite to methane with anaerobic microorganisms.[34,35] It indicates that electrostatic fields enrich the bulk medium with EAM, and drive bDIET for methane production.[36] The electrostatic field-driven DIET in the bulk medium is not proportional to the electrode surface area, with fewer electrode-related issues.

Interestingly, it was recently found that both polarized bioelectrodes and electric fields promote DIET through conductive materials in anaerobic reactors.[26,27,37] This implies that methane production can be maximized by adding a conductive material to the anaerobic reactor and applying a polarized bioelectrode or electrostatic field. Therefore, it is necessary to elucidate the characteristics of DIET promoted by polarization electrodes or electrostatic fields in anaerobic reactors with conductive materials and discuss their advantages and limitations.

In this study, in an anaerobic batch reactor with powdered activated carbon as a conductive material, the characteristics of methane production depending on the polarized bioelectrode and electrostatic field were investigated based on the electron transfer pathway, residual substrate, bioelectrochemical activity, substrate conversion, and microbial community.

RESULTS AND DISCUSSION

Activated Carbon Mediated DIET for Methane Production. Cumulative methane production in AC, an anaerobic batch reactor with powdered activated carbon, increased in the form of a sigmoidal curve with time (Figure 1). The methane production was saturated to 332.2 mL, higher than the control without the activated carbon. In anaerobic reactors, conductive materials, including activated carbon,

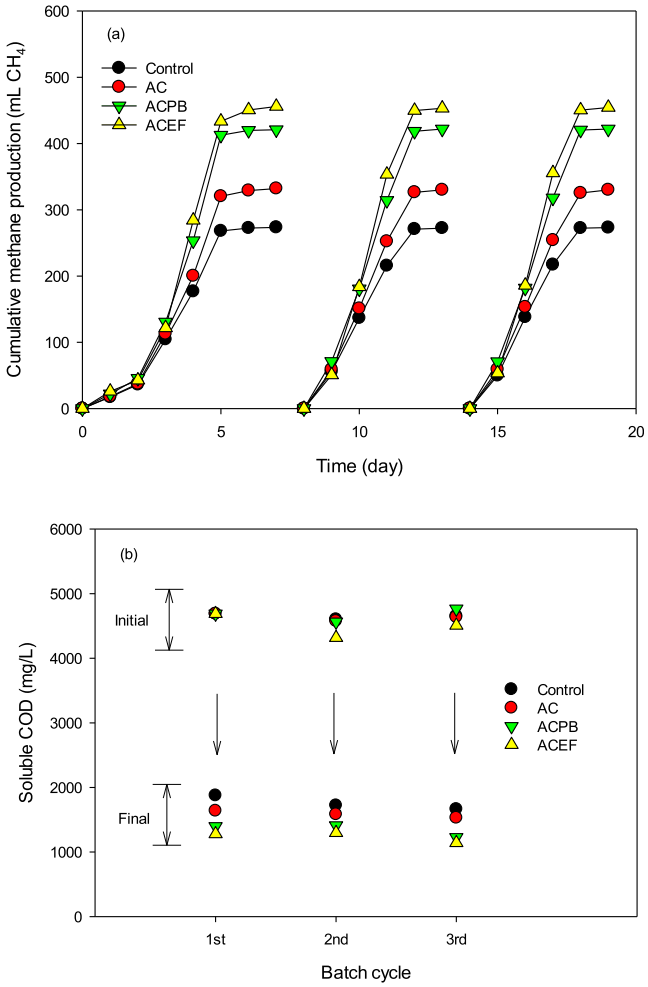

Figure 1. (a) Cumulative methane production and (b) soluble COD.

carbon cloth, carbon nanotube, graphene, and magnetite, can enrich the surface with EAM and serve as a conduit for cDIET for methane production.[14,15,38] In AC, the initial lag time required for substantial methane production was not considerably different from that of the control (Table 1). This suggests that anaerobic microorganisms quickly adhere to the surface of activated carbon particles in AC, express their electroactive genes for the thermodynamic benefits of cDIET over IIET, and promote methane production through cDIET. After repeating the batch cycle for AC, the methane yield was approximately 254.6 mL/g COD_r, 21.4% higher than the control (Table 1). The percentages of electron conversion from the substrate to methane for AC and control are 72.7 and 59.9%, respectively. In general, DIET improves methane yield over IIET by conserving the electrons better.[2,5,7] In methane production through IIET, electron conversion efficiency can be greatly affected by environmental factors such as temperature and pH and intermediate products and inhibitors.[4,6,8] In mesophilic conventional anaerobic digestion, the electron conversion from the substrate to methane ranged 35−75% in previous studies.[3,5] In control, the main electron transfer route for methane production may be IIET via the intermediates. Thus, the percentage of electron conversion for IIET can be considered as about 59.9% obtained from the control. On the other hand, the percentage of electron conversion between EAMs ranged from 70 to 96%, estimated from the Coulombic efficiency for methane production via the electrode in

https://doi.org/10.1021/acsomega.1c04108
ACS Omega 2021, 6, 29703−29712

Table 1. Features of Methane Productions Promoted by Activated Carbon and the Polarized Electrode

content	control	AC	ACPB	ACEF
λ (d)	0.60 ± 0.03	0.67 ± 0.01	0.74 ± 0.01	0.98 ± 0.01
μ_m (mL CH_4/d)	104.2 ± 0.6	122.8 ± 0.3	157.3 ± 1.2	196.4 ± 0.9
P_u (mL CH_4)	278.4 ± 0.1	337.8 ± 0.2	432.8 ± 0.1	462.5 ± 0.7
removed COD (g)	1.32 ± 0.02	1.32 ± 0.02	1.39 ± 0.01	1.45 ± 0.01
CH_4 yield (mL/g COD_r)	209.8 ± 0.1	254.6 ± 0.1	310.7 ± 0.1	317.3 ± 0.4
electron conversion (%)	59.9	72.7	88.8	90.7
DIET (%)	-	≤35.5	≤80.1	≤85.3
DIET rate (10^{-7} e^- moles/s)	0	1.80	5.21	6.93
remained soluble COD (mg/L)	1753 ± 108.5	1583.7 ± 55.0	1344.0 ± 101	1238.5 ± 84.7

MECs.[3,25] Thus, assuming that the contribution of DIET to methane production was 96% of the electron conversion, the percentage of cDIET contributing to methane production in AC can be roughly estimated as 35.5% ($96x + 59.9(100 - x) = 100 \times 72.7$, $x = 35.5$), based on the electron balance (eq 2). However, the contribution of DIET to methane production can increase further as the electron conversion (%) of DIET decreases. In a previous study using 1 g/L of activated carbon, the methane yield was 221.8 mL/g COD_r, and the percentage of cDIET was 7.8%, respectively, less than those in AC.[37]

It is well known that various conductive materials such as a carbon nanotube, carbon fiber, and iron/PANI complex improve methanogenesis by promoting extracellular electron transfer.[14,16] It seems that the contribution of cDIET to methane production depends on the properties of the conductive materials, such as specific surface area, electric conductivity, shape, and dose.[4,15,38] In AC, the maximum methane production rate was 122.8 mL/d, faster than the 104.2 mL/d for the control (Table 1). The increased methane production rate in AC appears to be related to more methane production.[4] Interestingly, at the end of each batch cycle, the residual of soluble COD in AC was slightly lower than that in control (Figure 1b), indicating that the substrate affinity of cDIET is higher than that of the IIET in anaerobic digestion. This confirms that cDIET is advantageous over IIET in kinetics and thermodynamics for methane production.[5,35,36]

Polarized Bioelectrode-driven DIET. In ACPB, the cumulative methane production increased over time in a pattern similar to that in AC (Figure 1a). However, the methane production increased to 432.8 mL, and the yield reached 310.7 mL/g COD_r, significantly higher than the AC (Table 1). The percentage of electron conversion from the substrate to methane in ACPB was 88.8%. The other fraction of electrons appears to be lost in the transfer process from the substrate to methane or used for microbial cell synthesis.[31,36] However, a small amount of methane dissolved in the liquid medium that was not recovered in a gaseous form may also be included in the lost electrons. The high methane yield in ACPB led to the improved maximum methane production rate of 157.3 mL/d, higher than the AC. The DIET fraction in methane production was estimated at up to 80.1% or more ($96x + 59.9(100 - x) = 100 \times 88.8$, $x = 80.1$), significantly higher than 35.5% of the cDIET alone in AC (Table 1). This suggests that DIET significantly contributed to improving methane production in ACPB. ACPB is a kind of single-chamber MECs containing activated carbon. In MECs, the electric potential on polarized electrodes drives eDIET for methane production by enriching the electrode surface with EAM.[15,25] Herein, it is noted that the polarized electrode potentials in MECs create an electrostatic field in the bulk solution. The electrostatic field may enrich the bulk solution with EAM.[5,32−37] Thus, it is believed that bDIET in the bulk solution also contributed to methane production in ACPB.[5] However, in ACPB, the methane yield of 310.7 mL/g COD_r was slightly higher than that of MECs without activated carbon in the previous study.[5] This indicates that the powdered activated carbon in ACPB has played an essential role in improving the methane yield. Conductive materials have been found to promote cDIET in MECs.[15] It seems that the electrostatic fields can polarize the surface of activated carbon particles, transforming them into small bipolar electrodes.[39,40] The polarized potentials on the bipolar activated carbon particles in ACPB may have enriched the surface with EAM and promoted the cDIET. Although it is still necessary to study further to estimate the individual DIET contributed to methane production in ACPB, at least three DIET types, namely, eDIET, cDIET, and bDIET appear to improve the methane production of ACPB, compared to that of the AC. In addition, at the end of each batch cycle, the residual of soluble COD in ACPB was lower than in AC (Figure 1b). This suggests that the more methane production in ACPB than in AC was due to higher methane yield and more substrate conversion.

Electrostatic Field-Driven DIET. In ACEF, the methane production was more interesting than in AC or ACPB. Cumulative methane production in ACEF was gradually saturated at 462.5 mL over time, higher than the ACPB (Figure 1a). ACEF is an anaerobic reactor that is similar to ACPB with powdered activated carbon and polarized bioelectrodes. However, the electrodes in ACEF were electrically insulated by coating their surface with a dielectric polymer film. The dielectric film on the electrode surface blocks the eDIET from transferring electrons for methane production. Nevertheless, the methane yield of ACEF was 317.3 mL/g COD_r, slightly higher than that of the ACPB, and the electron conversion from the substrate to methane was as high as 90.7% (Table 1). In ACEF, although the eDIET was excluded, the activated carbon and the electrostatic field were still involved in the electron transfer for methane production. Based on the electron balance, the contribution of DIET for methane production in ACEF was estimated as 85.3% or more ($96x + 59.9(100 - x) = 90.7 \times 100$, $x = 85.3$), higher than the AC or the ACPB. Compared to in AC, this can be direct evidence that the electrostatic field promoted bDIET and cDIET for methane production in ACEF. Also, in ACEF, the contribution of DIET being higher than in ACPB provides detailed information on the electron transfer for methane production. First, the electron transfer loss for eDIET is higher than that for bDIET or cDIET. Second, when eDIET is blocked, the electric field further improves bDIET and cDIET.

https://doi.org/10.1021/acsomega.1c04108
ACS Omega 2021, 6, 29703−29712

The electron transfer losses in the bioelectrochemical system are generally due to activation, ohmic, and concentration overpotentials.[5,35,41,42] The activation overpotential is the potential to overcome the activation energy for electron transfer. The overpotentials for bDIET are primarily related to the ability of EAM species to engage in extracellular electron transfer. The ohmic resistance of conductive materials, electrodes, or the electrode−wire interface may also interfere with the electron transfer, especially eDIET or cDIET.[5,41,42] The concentration overpotential is related to the mass transfer limiting the electron transfer. The higher electron losses in ACPB than in ACEF are likely due to the high ohmic resistances related to the electrode or the electrode−wire interface. There seems to be a difference in the thermodynamic potential to induce electron transfer between each DIET. The residual soluble COD in ACEF at the end of each batch cycle was 1238.3 mg/L, slightly lower than in ACPB (Figure 1b). As the contribution of DIET increases, the methane yield and substrate conversion appear to increase. It can be concluded that surface insulated electrodes, rather than polarized bioelectrode, selectively promote bDIET and cDIET by providing an electrostatic field to the bulk solution, thereby improving methane production.

Bioelectrochemical Activities in the Bulk Solution. The cyclic voltammogram (CV) for the bulk solution shows one oxidation and two reduction peaks under non-turnover conditions, similar to all anaerobic reactors (Figure 2a). The redox peaks of the CV indicate electrochemically active substances that include biotic and abiotic redox substances.[32,36,37,43] EEB and EMA belong to the biotic redox substances, and there are several types of abiotic substances, including flavins, quinones, and humic substances.[5,31] The redox peak potentials for EEB and EMA are known to be in the range −0.20 to 0.41 V versus Ag/AgCl and −0.07 to −0.41 V versus Ag/AgCl, respectively.[5,34,36] For AC, the oxidation peak was 0.01 V versus Ag/AgCl, and there were two reduction peaks at 0.17 and −0.38 V versus Ag/AgCl. The oxidation peak and the second reduction peak appeared to be the activities of EEB and EMA, based on their reported potential ranges (Figure 2a). The peak potentials for ACPB and ACEF were similar to those of AC. These similar bioelectrochemical properties in the anaerobic reactors appear to be caused by the activated carbon. In control, the redox peaks may be due to abiotic substances that are unable to mediate DIET. For AC, the peak heights for the oxidation and reduction were 0.50 and 0.57 mA, respectively. The peak heights for ACPB were higher than those for AC, and further for ACEF (Table 2). The peak height of CV indicates the abundance of EAM in the bulk solution.[5,34] This indicates that in AC, ACPB, and ACEF, EAM improved methane production by promoting DIET.

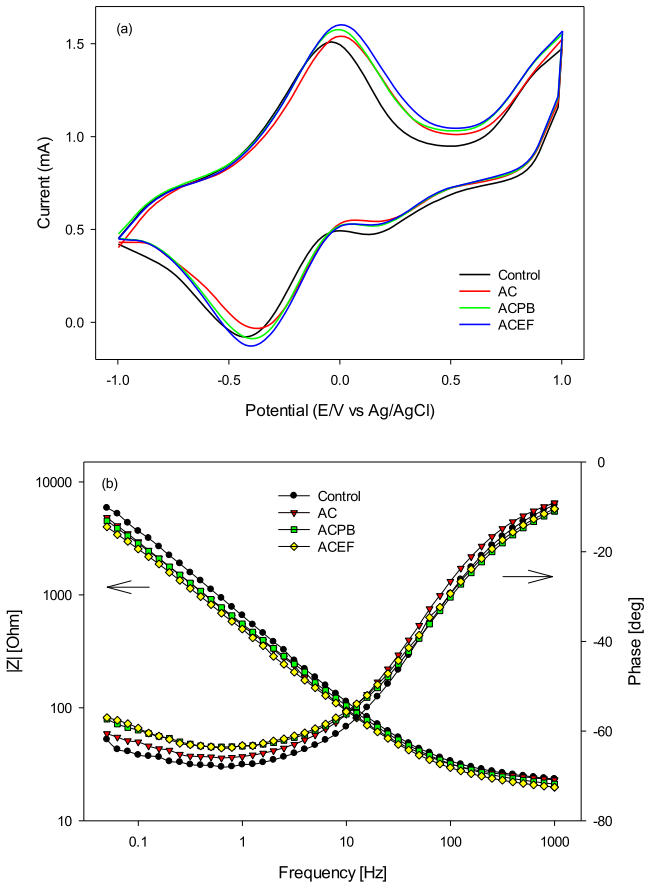

Figure 2. Electrochemical properties of the bulk solution: (a) CVs and (b) EIS curves.

The biotic and abiotic redox substances are known to be electrically conductive.[1,34,37] Thus, the conductivity or resistance of the bulk solution of bioelectrochemical reactors can be another indicator of the abundance of redox substances.[37] The solution resistance estimated from the electrochemical impedance spectrum (EIS) data was 21.5 Ω for control, and slightly decreased in the order AC > ACPB > ACEF (Table 2). The solution resistances were well matched with the redox peak heights in the CV. The activation overpotential for DIET can be informed from the charge transfer resistance of EAM. In control, the charge transfer resistance was very high at 3626.0 Ω (Table 2). This clearly shows the absence of EAM in control, and that even abiotic substances cannot mediate DIET.

The charge transfer resistance for the AC was 61.0 Ω, significantly smaller than for control. This means that the activated carbon surface was enriched with EAM in AC, and then methane production was promoted by cDIET. It is known that conductive materials could replace the pili or c-type cytochrome required for DIET in anaerobic digestion.[4,38] However, the force driving cDIET between EEB and EMA on conductive materials is still unclear. One hypothesis that could explain the driving mechanisms of cDIET is a local polarization of conductive materials. EEB transfers electrons to conductive materials for thermodynamic benefits. The electrons transferred from EEB can locally polarize the conductive materials. In addition, the electric potential of conductive materials can be locally positive by donating electrons to EMA for methane production. These local polarizations of conductive materials may induce direct electron transfer from EEB to EMA. However, further studies are needed to prove the hypothesis to describe the mechanisms of cDIET induction. The charge transfer resistances for ACPB and ACEF were further reduced to 51.9 and 47.5 Ω, respectively, compared to AC. ACPB and ACEF are the anaerobic reactors exposed to the electrostatic field. It can be concluded that the electrostatic field of ACPB and ACEF further enriches the bulk solution and activated carbon surface with EAM, promoting bDIET and cDIET for methane production.

Microbial Communities. The microbial samples collected from the bulk solution were taxonomically profiled based on

https://doi.org/10.1021/acsomega.1c04108
ACS Omega 2021, 6, 29703−29712

Table 2. Electrochemical Properties in CV and EIS for the Bulk Solution

content		control	AC	ACPB	ACEF
$E_{p,ox}/I_{p,ox}$ (V/mA)		−0.04/0.51	0.01/0.53	0.01/0.54	0.01/0.60
$E_{p,red1}/I_{p,red}$ (V/mA)		0.13/0.13	0.17/0.10	0.15/0.12	0.16/0.10
$E_{p,red2}/I_{p,red}$ (V/mA)		−0.42/0.53	−0.38/0.57	−0.39/0.60	−0.39/0.61
equivalent circuit for EIS	R_s (Ω)	21.5	21.1	19.1	18.1
R_s−Ql(R_{ct}−W)−ClR	Q_y	6.14×10^{-4}	3.33×10^{-4}	3.03×10^{-4}	3.40×10^{-4}
	Q_a	7.08×10^{-1}	8.24×10^{-1}	8.17×10^{-1}	8.18×10^{-1}
	R_{ct} (Ω)	3626.0	61.0	51.9	47.5
	W (Ω/$\sqrt{s}$)	2.21×10^{-5}	1.61×10^{-4}	2.05×10^{-4}	2.31×10^{-4}
	C (F)	6.80×10^{-4}	7.38×10^{-5}	8.20×10^{-5}	9.44×10^{-5}
	R (Ω)	19,950.9	3.2	3.5	3.3
	r^2	0.9998	0.9998	0.9997	0.9995

Table 3. Valid Reads, OTUs, and Diversity Indices for the Microbial Samples Collected from the Bulk Solution (Control, AC, ACPB, and ACEF)

indices		valid reads	OTUs	Ace	Chao1	NPShannon	Simpson
control	bacteria	33,237	1674	1807.9	1724.4	4.72	0.045
	archaea	73,546	95	104.3	98.9	1.32	0.446
AC	bacteria	31,301	1771	1913.2	1820.3	4.97	0.033
	archaea	80,177	171	182.2	173.8	2.64	0.101
ACPB	bacteria	29,191	1733	1893.1	1791.0	5.22	0.023
	archaea	73,372	174	178.8	175.1	2.63	0.106
ACEF	bacteria	28,520	1571	1714.4	1620.8	4.71	0.049
	archaea	70,969	153	163.5	156.3	2.59	0.110

the NGS platform. The valid reads for the archaea were significantly higher than that for the bacteria, but the operational taxonomic units (OTUs) were higher in bacteria (Table 3). For archaeal species, the richness (ACE, Chao1) and evenness (NPShannon, Simpson) in AC were significantly higher than in the control, but slightly lower in ACPB than the AC, further in ACEF (Table 3). It seems that activated carbon enriches the bulk solution or its surface with the archaeal species, and the polarized bioelectrodes and the electric field select the species. The effect of activated carbon, the polarized electrode, and the electric field on the richness of bacterial species was weaker than that of archaea, but it was not evident in the species evenness.

Of the OTUs identified bacterial taxa, *Streptococcus* and *BBZD_g* were commonly abundant bacteria at the genus level in all reactors (Figure 3a). However, *Porphyromonadaceae_uc*, *AJ009469_g*, and *Cloacamonas* were more abundant in AC, ACPB, and ACEF, than in control. The biplot obtained from principal component analysis (PCA) shows that the bacterial communities have similarities in AC, ACPB, and ACEF containing the activated carbon (Figure 4a). The species *Streptococcus henryi* and uncultured species *GQ458215_s*, *BBZD_g_uc*, and *AB234269_s* were the most abundant in control.

However, *Porphyromonadaceae_uc* and *Cloacamonas acidaminovorans* were more abundant bacterial species in AC, ACPB, and ACEF than control. The family Porphyromonadaceae is an obligately anaerobic fermenter producing acetate.[43] *C. acidaminovorans* is a synergistic species in an anaerobic digester degrading the acetate and propionate.[3] The species *Porphyromonadaceae_uc* and *C. acidaminovorans* are likely to be the EEB mediating DIET, which is frequently observed in bioelectrochemical systems.[5,43] *S. henryi* and *CU921187_s* were more abundant species in ACEF than the others. *S. henryi* is a facultative anaerobic fermenter, but appears to be an electroactive species that is commonly observed in bioelectrochemical systems.[5,44] *CU921187_s* is an uncultured bacterial species isolated from a mesophilic anaerobic digester for municipal wastewater sludge, abundant in the bioelectrochemical system for the methane conversion of coal.[35,45] It seems that *S. henryi* and *CU921187_s* are also EEB species that promote DIET in the electrostatic field. *Clostridium quinii* was an abundant bacterial species in AC and ACEF and is a commonly observed EEB species in bioelectrochemical systems.[5,36]

In archaeal groups, a clear difference in the dominant groups appeared at the genus level. Genus *Methanocorpusculum* was the predominant group in control. However, genera *Methanobacterium*, *Methanosaeta*, *LNJC_g*, and *Methanomassiliicoccus* were abundant in AC, and more in ACPB and ACEF (Figure 3b). As in the bacterial community, the archaeal community in AC was similar to those in ACPB and ACEF, but significantly different from that in control (Figure 4b). At the species level, *Methanocorpusculum_uc* and *Methanocorpusculum labreanum* were the predominant archaea in control. However, the five archaeal species, including *Methanobacterium palustre*, *Methanomassiliicoccus_uc*, *Methanosaeta concilii*, *LNJC_s*, and *Methanobacterium subterraneum*, were abundant in common in AC, ACPB, and ACEF. It is well known that *M. concilii* is an acetoclastic methanogen, and the other archaeal species are hydrogenotrophic methanogens.[5,10] However, these five archaeal species seem to be EMAs or syntrophic microbes involved in DIET commonly observed in bioelectrochemical anaerobic systems.[5,10,35,36,45] This suggests that the activated carbon enriches its surface with EMA, and the electrostatic field selects the microbial species to drive DIET for methane production.

Implications. The performance and stability of anaerobic digestion for organic matter significantly depend on the IIET, such as IIET and DIET, between acidogenic bacteria and

https://doi.org/10.1021/acsomega.1c04108
ACS Omega 2021, 6, 29703−29712

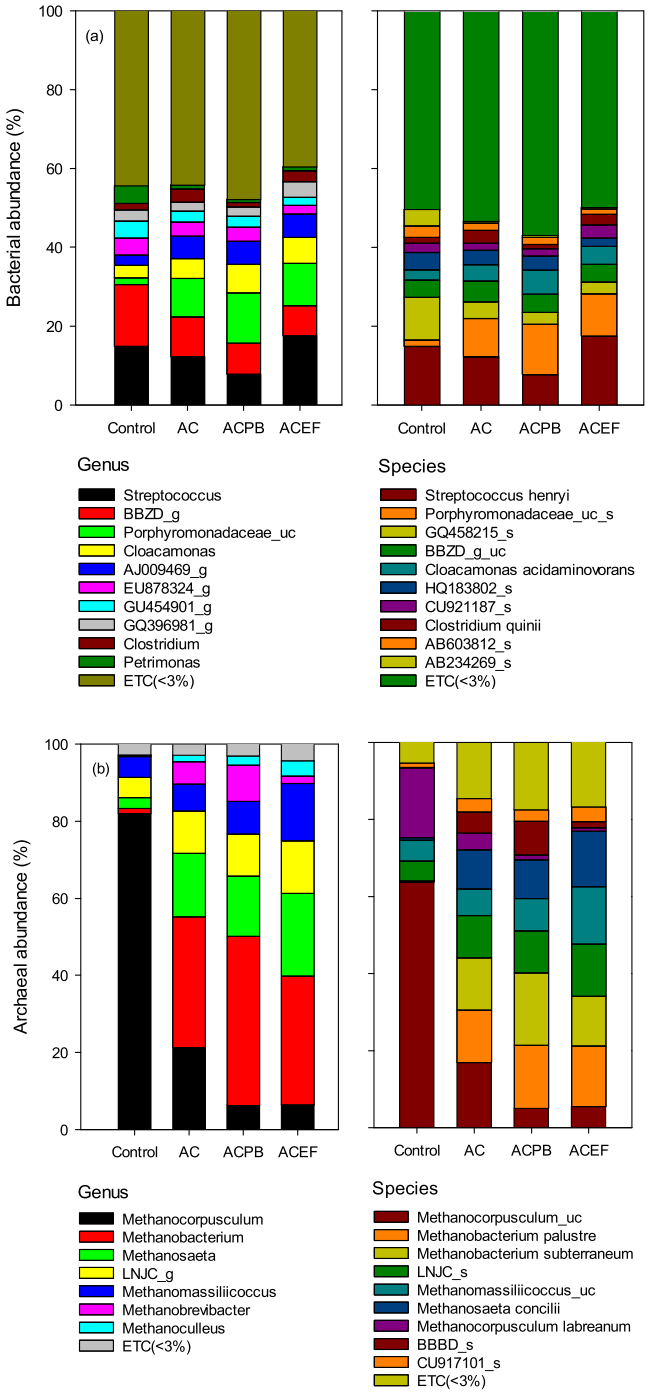

Figure 3. Abundance of microbial species (a) bacteria and (b) archaeal.

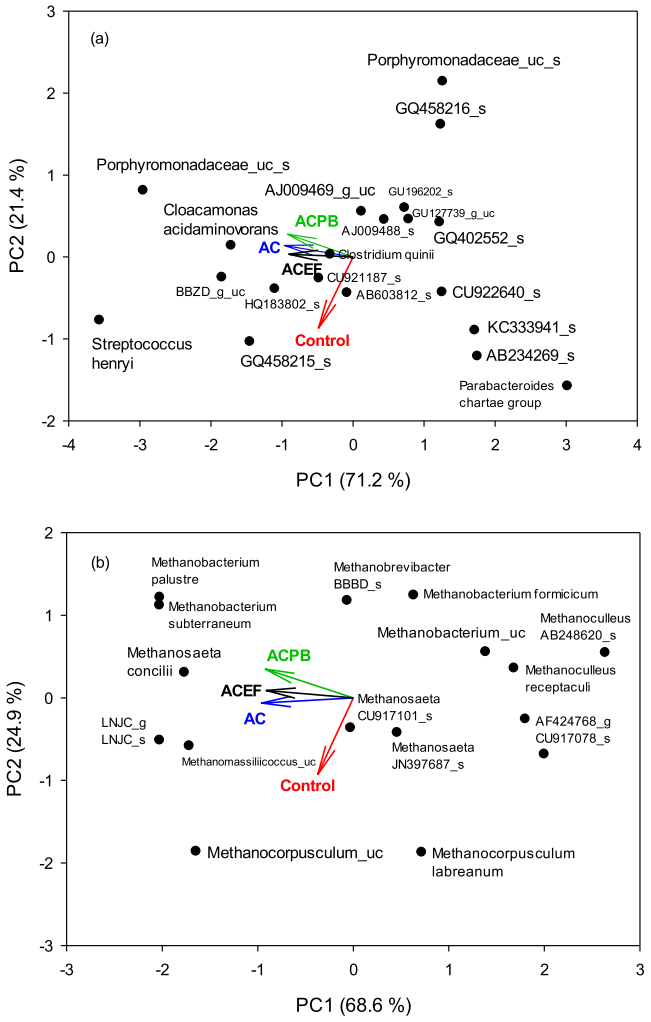

Figure 4. (a) Biplot for the bacterial communities and (b) Biplot for the archaeal communities.

methanogenic archaea.[1,2] In conventional anaerobic digestion, the main electron transfer pathway for methane production is IIET, in which various enzymatic reactions are involved.[2,5,29] Control is a conventional anaerobic digestion reactor. The methane yield of control based on the removed COD was as small as 209.8 mL/g COD_r. This indicates that during IIET for methane production, a significant amount of electrons are lost.[2,5,7]

It is well known that compared to IIET, DIET between EEB and EMA better conserves electrons and produces more methane.[7,29,36] Conductive materials, polarized electrodes, and direct electrical connection between EEB and EMA have been found to induce DIET.[5,25,38] In AC, the methane yield was 254.6 mL/g COD_r, which was higher than in control. AC is an anaerobic reactor that contains powdered activated carbon as a conductive material. This indicates that the activated carbon enriched EAM on its surface and mediated cDIET, consistent with the previous studies.[37,38] The contribution of DIET to methane production in AC was 35.5% or more depending on the electron conversion (%) of DIET, but the electron loss in AC was still high at 27.3% (Table 1). In anaerobic digestion, it has been thought that EMA improves methane production by reducing carbon dioxide with electrons transferred through conductive materials.[8,26,38] However, it revealed that the exoelectrogenic activity of microorganisms also contributes significantly to acetate dismutation for methane production in anaerobic digestion with conductive materials.[17−19] It is believed that the methane yield in AC could be further improved by understanding the cDIET mechanism for methane production. However, how conductive materials enrich EAM and mediate cDIET is still not well explained. Herein, a local polarization of conductive materials was proposed to describe the driving mechanism of cDIET.

In MECs, EEB oxidizes low molecular organics on the polarized bioanode surface.[5,15,25] The electrons move to the biocathode through the external circuit and combine with carbon dioxide to produce methane. ACPB is a kind of single-

https://doi.org/10.1021/acsomega.1c04108
ACS Omega 2021, 6, 29703−29712

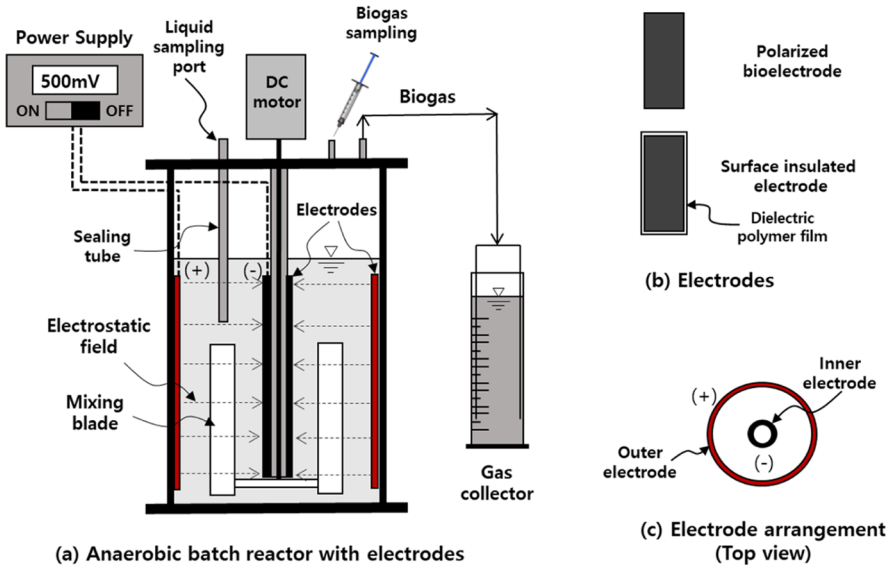

Figure 5. (a) Schematic diagram of the bioelectrochemical anaerobic batch reactor. (b) Prepared electrodes. (c) Electrode arrangement.

chamber MECs with activated carbon in the bulk solution. In ACPB, the methane yield was 310.7 mL/g COD_r, significantly higher than that of AC, and the contribution of DIET to methane production was 80.1% or more (Table 1). It is considered that activated carbon-induced cDIET and polarized bioelectrodes-driven eDIET in ACPB have improved the methane yield. However, in the anaerobic reactor with polarized electrodes, EAMs, including EEB and EMA, were abundant in the bulk solution and the polarized electrode surface.[5,29] bDIET also appears to have contributed to the high DIET in ACPB. However, MECs, including ACPB, have some limitations in their practical applications.[36] First, the polarized bioelectrode continuously consumes electric power to maintain the Faradaic current for methane production. Second, organic matter oxidation and carbon dioxide reduction for methane production are expected only on the bioanode and biocathode surfaces, respectively. This indicates that the DIET for methane production depends on the surface area of polarized bioelectrodes. However, the electrode with sufficient area can interfere with agitation and increase the initial capital cost for bioelectrochemical systems. Third, polarized bioelectrodes can quickly deteriorate in the anaerobic digestion environment, increasing the maintenance cost to replace the electrode periodically.

In the case of ACEF, the electrodes were insulated by coating the surface with a dielectric material. Thus, the electrode polarization creates the electrostatic field in the bulk solution, but there is no Faradaic current through the electrode surface. The only DIETs that can be expected in ACEF are cDIET and bDIET. Interestingly, the methane yield in ACEF was 317.3 mL/g COD_r, higher than that in ACPB, and the contribution of DIET to methane production was 85.3% or more (Table 1). The electron transfer loss of eDIET appears to have been more significant than that of cDIET or bDIET. In the case of ACPB, the electrode or wire connection part involved in eDIET may have high ohmic resistance.[41] This means that the electrostatic field further improved cDIET and bDIET selectively in the bulk solution, consistent with the previous studies.[35−37] The electrostatic field-driven DIET can be explained by the Lorentz force that moves electrons, polar molecules, and charged ions.[28] However, in redox reactions, the electron transfer under electrostatic fields can also be described based on thermodynamics.[46] The equilibrium constant (K) for a redox reaction depends on the free energy change ($\Delta G = -RT \times \ln K$, where R is the ideal gas constant, and T is the absolute temperature). The free energy (G) is a function of enthalpy (H), entropy (S), and temperature (T) ($G = H - TS$). The electrostatic field changes the enthalpy and entropy by changing the molecular polarity, bridging the charged particles, or oscillating the permanent dipole.[46−48] This suggests that the electrostatic field reduces the activation energy required to be the transient state, providing the kinetic advantages to the electron transfer for the redox reaction, promoting DIET.[48,49]

In AC, the DIET rate, estimated from the maximum methane production rate, was 1.80×10^{-7} e^- moles/s (Table 1). However, the polarized bioelectrode increased the DIET rate by 2.89 times compared to AC, and the electric field in ACEF further improved by 3.85 times. In anaerobic digestion, the electrostatic field-promoted cDIET and bDIET have several advantages over eDIET via polarized bioelectrode. First, the electrostatic field can be created with relatively small surface areas of polarized electrodes. Second, the electrode surface can be coated with a durable dielectric polymer to extend its life. This means that the electrostatic field in the bulk solution can be somewhat free from the limitations due to electrode size or electrode material. Third, the surface-coated electrodes do not directly consume DC electric power to create the electrostatic field. However, electrostatic fields further increase the contribution of DIET to methane production compared to polarized bioelectrodes. It is noted that as the DIET contribution for methane production increases, the methane yield and substrate conversion increase, significantly improving the overall methane production. Therefore, the electrostatic field-promoted DIET can be a new bioelectrochemical platform that economically improves anaerobic digestion performance.

CONCLUSIONS

Activated carbon in anaerobic reactors enriches the surface with EAMs, improving methane production through cDIET. In anaerobic reactors with activated carbon, polarized electrodes

https://doi.org/10.1021/acsomega.1c04108
ACS Omega 2021, 6, 29703−29712

enrich EAMs on the surfaces of the electrode and activated carbon and in the bulk solution, improving methane production by eDIET, cDIET, and bDIET. The surface insulation of the electrode blocks eDIET, but the electrostatic field further promotes cDIET and bDIET selectively in the bulk solution to improve methane production. When applied to large-scale anaerobic reactors, the electrostatic field has many advantages over polarized bioelectrodes in promoting DIET for methane production. Thus, the anaerobic digestion, combined with an electrostatic field, is a viable bioelectrochemical platform that can apply to field-scale anaerobic digestion.

MATERIALS AND METHODS

Anaerobic Medium and Seed Sludge. An artificial anaerobic medium containing 6.0 g/L glucose, 8.4 g/L $NaHCO_3$, 4.9 g/L NaH_2PO_4, 9.16 g/L Na_2HPO_4, 0.62 g/L NH_4Cl, 0.62 g/L KCl, 20 mL/L vitamins, and 10.0 mL/L trace minerals was prepared, as described in previous studies.[5,35,36] Powdered activated carbon as a conductive material was obtained from a local provider (Power Carbon Technology Co., Ltd., Korea, size 5−10 μm, surface area 1600−2200 m^2/g, ash content <0.1%, electric conductivity <600 μS/cm). The anaerobic digestion sludge was collected from a mesophilic anaerobic digester for a waste-activated sludge in a municipal wastewater reclamation center (S-MWTP, Busan, Korea), then used as the seed sludge after screening with 1.0 mm sieve to remove impurities. The initial values of pH, alkalinity, and volatile suspended solids (VSSs) of the seed sludge were 7.63, 5,133 mg/L as $CaCO_3$, and 17,880 mg/L, respectively.

Anaerobic Batch Reactor. An anaerobic batch reactor (effective volume, 0.5 L; diameter, 8.5 cm) was prepared with a tube of cylindrical acrylic resin (Figure 5a). The reactor was sealed with an acrylic cover plate, and a blade was installed inside the reactor to mix the anaerobic medium. The blade was connected to a DC motor located on the cover plate using a steel shaft. Three ports for biogas sampling, biogas venting, and liquid medium sampling were placed at the cover plate, respectively. The biogas sampling ports were sealed with an n-butyl rubber stopper. Two sealing tubes extended to inside the liquid medium were attached to the port bottoms for liquid sampling and steel shaft passage to block the gas flow between inside and outside the reactor. The biogas venting port was connected to a floating-type gas collector using a rubber tube.

The electrodes were prepared by cutting a titanium foil (BJHYD Nonferrous Metal Materials Co., China) into small (17.3 × 7 cm) and large (81.6 × 9 cm) sizes (Figure 5b). The small and large electrodes were installed in an annular shape on the steel-shaft tube outer wall and the reactor-inner wall, respectively (Figure 1a,c). Powdered activated carbon was added to be 3.0 g/L into the reactor with the electrodes, and called ACPB. The surface-insulated electrodes were also prepared by coating the titanium foil electrode surfaces with a dielectric polymer (Alkyd enamel, NOROO Paint & Coatings Co., Ltd., Korea). The surface-insulated electrodes were installed in another anaerobic reactor called ACEF in the same way as ACPB. The electrodes installed in the reactors, ACPB and ACEF, were connected to an external DC voltage source (OPM series, ODA Technologies Co., Incheon, Korea) using titanium wires. The anaerobic medium (0.25 L), the inoculum (0.25 L), and powdered activated carbon (1.5 g) were added into the reactors, and then flushed with nitrogen gas to remove oxygen from the anaerobic reactor. The electrodes were polarized by applying 0.5 V between the anode and cathode using the DC voltage source. The electrostatic field exposed to the bulk solution averaged 0.17 V/cm. The anaerobic medium in the reactor was mixed with the blade in a temperature-controlled room at 35 ± 2 °C.

The anaerobic batch reactor called AC containing the activated carbon (3 g/L) was also prepared in the same procedure as ACPB, except for the electrode-related parts. Another anaerobic batch reactor without the activated carbon and the electrodes was prepared separately as the control. A blank anaerobic batch reactor without the substrate was also prepared to correct the biogas production from the seed sludge. All anaerobic batch reactors were operated in sequential batch mode over three batch cycles by precipitating suspended microorganisms when no biogas production was observed, and replacing the supernatant with a fresh medium.

Analysis and Calculation. The biogas production was intermittently monitored with a floating-type gas collector. The biogas composition was analyzed by gas chromatography (Gow-Mac Instrument Co., PA, USA), which was equipped with a Porapak-Q column (6 ft × 1/8 in, SS) and thermal conductivity detector. The methane production between monitoring time intervals was estimated from the total biogas volume and methane content, as described in previous studies.[35,36] The methane production was converted to the value at standard temperature and pressure, after correcting methane production from the seed sludge. The cumulative methane production over time was fitted to the modified Gompertz equation (eq 1) using the nlstool package in *R*, and the parameters, including initial lag time (λ, days), maximum methane production rate (μ_m, mL/d), and ultimate methane production (P_u, mL), were obtained[5,36,37]

$$P = P_u \times \exp\left[-\exp\left(\frac{\mu_m \times \exp(1)}{P_u}(\lambda - t) + 1\right)\right] \quad (1)$$

The methane yield was calculated by dividing the ultimate methane production (P_u, mL CH_4) by the COD removal (g). The percentage of electron conversion to methane from the substrate was obtained by dividing the methane yield by the theoretical value (350 mL/g COD_r). The contribution of DIET to methane production was estimated based on a simple electron balance equation (eq 2), as described in a previous study[36]

$$ax + by = 100c \quad \text{and} \quad x + y = 100 \quad (2)$$

where, x and y are the percentages (%) of DIET and IIET contributing to methane production, respectively. The constants, a and b, are the electron conversions (%) from the substrate to methane for DIET and IIET, and c is the overall electron conversion (%). Assuming that carbon dioxide is reduced with electrons transferred through DIET to produce methane, the number of electron moles (n) transferred to produce 1 mol of methane is 8. Therefore, the electron transfer rate (ETR, e^- moles/s) for DIET was estimated from the maximum methane production rate (μ_m), the DIET percentage (x), and the number (n) of electron moles. The changes in chemical properties, including pH, alkalinity, COD, and VSS, were also measured at the beginning and end of each batch cycle. For the bulk solution, the CV was obtained at the potential range −1.0 to 1.0 V (relative to the Ag/AgCl reference electrode) at the scanning rate 10 mV/s. A pair of small stainless-steel mesh pieces (1 × 1 cm) were used as the

https://doi.org/10.1021/acsomega.1c04108
ACS Omega 2021, 6, 29703−29712

working and counter electrodes.[36] Smart Manager (ZIVE BP2 series, WonATech Co., Ltd., Korea) was used to obtain the peak height and potential from the CV. The EIS was also obtained with an alternating current signal amplitude of 25 mV in the frequency band of 0.01−1000 Hz using the electrochemical instrument (ZIVE SP1, WonATech Co., Ltd., Korea).[5] The EIS data were fitted into an equivalent circuit model using software (ZMAN 2.4, ZIVE LAB, WonATech Co., Ltd., Korea). The equivalent circuit model consisting of three components of the impedances connected in series, (R_s−Q|(R_{ct}−W)−C|R), was used. The impedance components were (i) a solution resistance (R_s), (ii) a constant phase element (Q) in parallel with a series of charge transfer resistance (R_{ct}) and the Warburg element (W), and (iii) a double-layer capacitor (C) in parallel with an ohmic resistance (R) of the electrode.

Microbial Taxonomic Profiling. Taxonomic profiling of metagenomic samples for the anaerobic batch reactors was performed to investigate the 16S rRNA of microbial communities at the end of the experiment. According to the kit protocol (MO BIO Laboratories, Inc., CA, USA), the DNA was extracted from the suspended microorganisms in the bulk solution using the Power Soil DNA isolation kit. The fusion primer was used to amplify the variable region (V3V4 for bacteria, V1V9 for archaea) of the 16S rRNA gene in the metagenomic DNA. The 16S rRNA was pooled and sequenced on the MiSeq Personal Sequencer (Illumina, San Diego, CA, USA). The amplification, construction of the sequencing library, and bioinformatics analysis were performed as described in previous studies.[32,36] Chimera was checked, and taxonomic assignments of these readings were conducted using the EzBioCloud database (http://ezbiocloud.net/). The microbial community and the statistical taxonomical assignments were obtained through the OTUs. Comprehensive bioinformatics analysis, such as species-level classification of microbes, cluster analysis, microbial origin tracking, hierarchical clustering, and various species diversity indicators, was conducted by the EZ Biocloud (Chunlab, Inc., Seoul, Korea). The microbial community data for the samples were statistically analyzed with PCA using the factoextra package in R. The properties of the bacterial and archaeal communities in the anaerobic reactors were estimated from the biplot in PCA.

AUTHOR INFORMATION

Corresponding Author

Young-Chae Song − *Department of Environmental Engineering, Korea Maritime and Ocean University, Busan 49112, Republic of Korea;* orcid.org/0000-0002-2416-4785; Phone: +82-10-7151-4417; Email: soyc@kmou.ac.kr

Authors

Hanchao Yu − *Department of Environmental Engineering, Korea Maritime and Ocean University, Busan 49112, Republic of Korea*

Byung-Uk Bae − *Department of Environmental Engineering, Daejeon University, Daejeon 34520, Republic of Korea*

Jun Li − *Institute of Engineering Thermophysics, School of Energy and Power Engineering, Chongqing University, Chongqing 400044, China;* orcid.org/0000-0002-1449-8810

Seong-Ho Jang − *Department of Bio-Environmental Energy, Pusan National University, Miryang 50463, Republic of Korea*

Complete contact information is available at: https://pubs.acs.org/10.1021/acsomega.1c04108

Notes

The authors declare no competing financial interest.

ACKNOWLEDGMENTS

This work was supported by a grant from the National Research Foundation (NRF) of Korea, funded by the South Korean Government (MSIP) [NRF-2017R1E1A1A01075325].

REFERENCES

(1) Shrestha, P. M.; Rotaru, A.-E. Plugging in or going wireless: strategies for interspecies electron transfer. *Front. Microbiol.* **2014**, *5*, 237.

(2) Shen, L.; Zhao, Q.; Wu, X.; Li, X.; Li, Q.; Wang, Y. Interspecies electron transfer in syntrophic methanogenic consortia: From cultures to bioreactors. *Renewable Sustainable Energy Rev.* **2016**, *54*, 1358−1367.

(3) Feng, Q.; Song, Y.-C.; Bae, B.-U. Influence of applied voltage on the performance of bioelectrochemical anaerobic digestion of sewage sludge and planktonic microbial communities at ambient temperature. *Bioresour. Technol.* **2016**, *220*, 500−508.

(4) Park, J.-H.; Kang, H.-J.; Park, K.-H.; Park, H.-D. Direct interspecies electron transfer via conductive materials: A perspective for anaerobic digestion applications. *Bioresour. Technol.* **2018**, *254*, 300−311.

(5) Feng, Q.; Song, Y.-C.; Ahn, Y. Electroactive microorganisms in bulk solution contribute significantly to methane production in bioelectrochemical anaerobic reactor. *Bioresour. Technol.* **2018**, *259*, 119−127.

(6) Bouraima, S.; Fagbemi, L. A.; Adamon, D. G. F. An efficient visible numerical model to find the optimal anaerobic digestion temperature in a continuous reactor without hydrolytic microbial compartment. *ES Energy Environ.* **2021**, *13*, 13−24.

(7) Lovley, D. R. Reach out and touch someone: potential impact of DIET (direct interspecies energy transfer) on anaerobic biogeochemistry, bioremediation, and bioenergy. *Rev. Environ. Sci. Biotechnol.* **2011**, *10*, 101−105.

(8) Blasco-Gómez, R.; Batlle-Vilanova, P.; Villano, M.; Balaguer, M.; Colprim, J.; Puig, S. On the edge of research and technological application: A critical review of electromethanogenesis. *Int. J. Mol. Sci.* **2017**, *18*, 874.

(9) Yang, Y.; Xu, M.; Guo, J.; Sun, G. Bacterial extracellular electron transfer in bioelectrochemical systems. *Process Biochem.* **2012**, *47*, 1707−1714.

(10) Rotaru, A.-E.; Shrestha, P. M.; Liu, F.; Shrestha, M.; Shrestha, D.; Embree, M.; Zengler, K.; Wardman, C.; Nevin, K. P.; Lovley, D. R. A new model for electron flow during anaerobic digestion: direct interspecies electron transfer to Methanosaeta for the reduction of carbon dioxide to methane. *Energy Environ. Sci.* **2014**, *7*, 408−415.

(11) Viggi, C. C.; Rossetti, S.; Fazi, S.; Paiano, P.; Majone, M.; Aulenta, F. Magnetite particles triggering a faster and more robust syntrophic pathway of methanogenic propionate degradation. *Environ. Sci. Technol.* **2014**, *48*, 7536−7543.

(12) Chabert, N.; Ali, O. A.; Achouak, W. All ecosystems potentially host electrogenic bacteria. *Bioelectrochem* **2015**, *106*, 88−96.

(13) Doyle, L. E.; Marsili, E. Methods for enrichment of novel electrochemically-active microorganisms. *Bioresour. Technol.* **2015**, *195*, 273−282.

(14) Kato, S.; Hashimoto, K.; Watanabe, K. Methanogenesis facilitated by electric syntrophy via (semi)conductive iron-oxide minerals. *Environ. Microbiol.* **2012**, *14*, 1646−1654.

(15) Yu, Z.; Leng, X.; Zhao, S.; Ji, J.; Zhou, T.; Khan, A.; Kakde, A.; Liu, P.; Li, X. A review on the applications of microbial electrolysis cells in anaerobic digestion. *Bioresour. Technol.* **2018**, *255*, 340−348.
(16) Hu, Q.; Zhou, J.; Qiu, B.; Wang, Q.; Song, G.; Guo, Z. Synergistically improved methane production from anaerobic wastewater treatment by iron/polyaniline composite. *Adv. Compos. Hybrid Mater.* **2021**, *4*, 265−273.
(17) Xiao, L.; Sun, R.; Zhang, P.; Zheng, S.; Tan, Y.; Li, J.; Zhang, Y.; Liu, F. Simultaneous intensification of direct acetate cleavage and CO2 reduction to generate methane by bioaugmentation and increased electron transfer. *Chem. Eng. J.* **2019**, *378*, 122229.
(18) Xiao, L.; Liu, F.; Lichtfouse, E.; Zhang, P.; Feng, D.; Li, F. Methane production by acetate dismutation stimulated by Shewanella oneidensis and carbon materials: An alternative to classical CO2 reduction. *Chem. Eng. J.* **2020a**, *389*, 124469.
(19) Xiao, L.; Zheng, S.; Lichtfouse, E.; Luo, M.; Tan, Y.; Liu, F. Carbon nanotubes accelerate acetoclastic methanogenesis: From pure cultures to anaerobic soils. *Soil Biol. Biochem.* **2020**, *150*, 107938.
(20) Liu, L.; Bernazzani, P.; Chu, W.; Luo, S.-Z.; Wang, B.; Guo, Z. Polyelectrolyte assisted preparation of nanocatalysts for CO2 methanation. *Eng. Sci.* **2018**, *2*, 74−81.
(21) Zhang, X.; Ziemer, K. S.; Weeks, B. L. Combustion synthesis of N-doped three-dimensional graphene networks using graphene oxide−nitrocellulose composites. *Adv. Compos. Hybrid Mater.* **2019**, *2*, 492−500.
(22) Gijare, M.; Chaudhari, S.; Ekar, S.; Garje, A. Reduced graphene oxide based electrochemical nonenzymatic human serum glucose sensor. *ES Mater. Manuf.* **2021**, *14*, 110−119.
(23) Mirabootalebi, S. O. A new method for preparing buckypaper by pressing a mixture of multi-walled carbon nanotubes and amorphous carbon. *Adv. Compos. Hybrid Mater.* **2020**, *3*, 336−343.
(24) Fallah, S.; Mamaghani, H. R.; Yegani, R.; Hajinajaf, N.; Pourabbas, B. Use of graphene substrates for wastewater treatment of textile industries. *Adv. Compos. Hybrid Mater.* **2020**, *3*, 187−193.
(25) Xafenias, N.; Mapelli, V. Performance and bacterial enrichment of bioelectrochemical systems during methane and acetate production. *Int. J. Hydrogen Energy* **2014**, *39*, 21864−21875.
(26) Kim, K.-R.; Kang, J.; Chae, K.-J. Improvement in methanogenesis by incorporating transition metal nanoparticles and granular activated carbon composites in microbial electrolysis cells. *Int. J. Hydrogen Energy* **2017**, *42*, 27623−27629.
(27) LaBarge, N.; Yilmazel, Y. D.; Hong, P.-Y.; Logan, B. E. Effect of pre-acclimation of granular activated carbon on microbial electrolysis cell startup and performance. *Bioelectrochemistry* **2017**, *113*, 20−25.
(28) Cheng, H.-M.; Wang, F.-M.; Chu, J. P. Effect of Lorentz force on the electrochemical performance of lithium-ion batteries. *Electrochem. Commun.* **2017**, *76*, 63−66.
(29) Feng, Q.; Song, Y.-C.; Yoo, K.; Kuppanan, N.; Subudhi, S.; Lal, B. Polarized electrode enhances biological direct interspecies electron transfer for methane production in upflow anaerobic bioelectrochemical reactor. *Chemosphere* **2018**, *204*, 186−192.
(30) Wang, D.; Han, H.; Han, Y.; Li, K.; Zhu, H. Enhanced treatment of Fischer-Tropsch (F-T) wastewater using the upflow anaerobic sludge blanket coupled with bioelectrochemical system: Effect of electric field. *Bioresour. Technol.* **2017**, *232*, 18−26.
(31) Joicy, A.; Song, Y.-C.; Lee, C.-Y. Electroactive microorganisms enriched from activated sludge remove nitrogen in bioelectrochemical reactor. *J. Environ. Manag.* **2019a**, *233*, 249−257.
(32) Joicy, A.; Song, Y.-C.; Yu, H.; Chae, K.-J. Nitrite and nitrate as electron acceptors for bioelectrochemical ammonium oxidation under electrostatic field. *J. Environ. Manag.* **2019b**, *250*, 109517.
(33) Tang, J.; Li, X.; Zhao, W.; Wang, Y.; Cui, P.; Zeng, R. J.; Yu, L.; Zhou, S. Electric field induces electron flow to simultaneously enhance the maturity of aerobic composting and mitigate greenhouse gas emissions. *Bioresour. Technol.* **2019**, *279*, 234−242.
(34) Piao, D.-M.; Song, Y.-C.; Kim, D.-H. Bioelectrochemical Enhancement of Biogenic Methane Conversion of Coal. *Energies* **2018**, *11*, 2577.
(35) Piao, D.-M.; Song, Y.-C.; Oh, G.-G.; Kim, D.-H.; Bae, B.-U. Contribution of yeast extract, activated carbon, and an electrostatic field to interspecies electron transfer for the bioelectrochemical conversion of coal to methane. *Energies* **2019**, *12*, 4051.
(36) Oh, G.-G.; Song, Y.-C.; Bae, B.-U.; Lee, C.-Y. Electric field-driven direct interspecies electron transfer for bioelectrochemical methane production from fermentable and non-fermentable substrates. *Processes* **2020**, *8*, 1293.
(37) Feng, Q.; Song, Y.-C.; Li, J.; Wang, Z.; Wu, Q. Influence of electrostatic field and conductive material on the direct interspecies electron transfer for methane production. *Environ. Res.* **2020**, *188*, 109867.
(38) Kouzuma, A.; Kato, S.; Watanabe, K. Microbial interspecies interactions: recent findings in syntrophic consortia. *Front. Microbiol.* **2015**, *6*, 477.
(39) Hwang, J. G.; Zahn, M.; Pettersson, L. A. A. Bipolar charging and discharging of a perfectly conducting sphere in a lossy medium stressed by a uniform electric field. *J. Appl. Phys.* **2011**, *109*, 084331.
(40) Koefoed, L.; Pedersen, S. U.; Daasbjerg, K. Review article bipolar electrochemistry-A wireless approach for electrode reactions. *Curr. Opin. Electrochem.* **2017**, *2*, 13−17.
(41) Choi, T.-S.; Song, Y.-C.; Timothy, H. A facile method for preparation of efficient oxygen reduction catalyst for a microbial fuel cell cathode. *KSCE J. Civ. Eng.* **2018**, *22*, 31−39.
(42) Storck, T.; Virdis, B.; Batstone, D. J. Modelling extracellular limitations for mediated versus direct interspecies electron transfer. *ISME J.* **2016**, *10*, 621−631.
(43) Schmidt, A.; Sturm, G.; Lapp, C. J.; Siebert, D.; Saravia, F.; Horn, H.; Ravi, P. P.; Lemmer, A.; Gescher, J. Development of a production chain from vegetable biowaste to platform chemicals. *Microb. Cell Factories* **2018**, *17*, 90.
(44) Milinovich, G. J.; Burrell, P. C.; Pollitt, C. C.; Bouvet, A.; Trott, D. J. Streptococcus henryi sp. nov. and Streptococcus caballi sp. nov., isolated from the hindgut of horses with oligofructose-induced laminitis. *Int. J. Syst. Evol. Microbiol.* **2008**, *58*, 262−6.
(45) Sato, K.; Kawaguchi, H.; Kobayashi, H. Bio-electrochemical conversion of carbon dioxide to methane in geological storage reservoirs. *Energy Convers. Manag.* **2013**, *66*, 343−350.
(46) Wisseroth, K. P.; Braune, H. Thermodynamic equilibrium in strong electric fields and field chemistry consequences. *J. Phys.* **1977**, *38*, 1249−1255.
(47) English, N. J.; Waldron, C. J. Perspectives on external electric fields in molecular simulation: progress, prospects and challenges. *Phys. Chem. Chem. Phys.* **2015**, *17*, 12407−12440.
(48) Pivrikas, A.; Ullah, M.; Sitter, H.; Sariciftci, N. S. Electric field dependent activation energy of electron transport in fullerene diodes and field effect transistors: Gill's law. *Appl. Phys. Lett.* **2011**, *98*, 092114.
(49) Dignam, M. J.; Gibbs, D. B. The electric field dependence of the net activation energy for migration of ionic species across an activation. *J. Phys. Chem. Solids* **1969**, *30*, 375−393.

https://doi.org/10.1021/acsomega.1c04108
ACS Omega 2021, 6, 29703−29712